NACA RM L54F29

NACA

RESEARCH MEMORANDUM

ASPECTS OF INTERNAL-FLOW-SYSTEM DESIGN FOR HELICOPTER PROPULSIVE UNITS

By John R. Henry

Langley Aeronautical Laboratory
Langley Field, Va.

NATIONAL ADVISORY COMMITTEE
FOR AERONAUTICS

WASHINGTON

September 14, 1954

NATIONAL ADVISORY COMMITTEE FOR AERONAUTICS

RESEARCH MEMORANDUM

ASPECTS OF INTERNAL-FLOW-SYSTEM DESIGN FOR HELICOPTER PROPULSIVE UNITS

By John R. Henry

SUMMARY

Pertinent items relating to the design of internal-flow systems for reciprocating engine, turbine engine, and pressure-jet installations in helicopters are discussed. The importance of the following items is emphasized: controllable exit and ram recovery for reciprocating-engine cooling; performance penalties possible in turbine-engine installations attributed to distortions in the flow distribution at the face of the axial compressor; the effects of high subsonic flow velocities on the performance of duct elements; and the effects of centrifugal forces on the flow in a ducted helicopter rotor. Data on the maximum flow capacities of bends are included.

INTRODUCTION

Helicopter performance requirements have pushed the flight speed range up from 100 mph to perhaps 150 to 200 mph. Such speed-range changes in the history of the conventional airplane influenced the design of ducting and air-cooling systems in certain respects. It is desirable to reexamine current and future helicopter designs and requirements to determine any design trends indicated by the increasing flight speeds. First, the reciprocating-engine cooling-system installations are examined and then the internal-flow problems related to other types of powerplant installations - for instance, the gas turbine - are discussed. The purpose of this paper is to touch on various pertinent items relating to internal flow, not to present a detailed set of design rules and data.

SYMBOLS

A	cross-sectional area, sq ft
a_0	speed of sound in free stream, ft/sec
C_p	pressure-rise coefficient

D	diameter of fan rotor or circular duct, as indicated
H	total pressure, lb/sq ft, abs
h	height of rectangular duct, ft
M	Mach number
n	fan rotational speed, rps
Q	volume flow, cu ft/sec
q_c	dynamic pressure corrected for compressibility
q_0	flight dynamic pressure
R	rotor-blade radius to tip, ft
r	radius (various radii are defined where used)
V_0	flight velocity relative to free stream, ft/sec except as indicated otherwise
V_X	exit velocity relative to helicopter, ft/sec
w	width of rectangular duct, ft
ΔH	total-pressure change, lb/sq ft
η	fan efficiency
ρ	mass density
Ω	angular velocity of rotor blade, radians/sec

Subscripts:

C	cooler
D	duct
F	fan
1	at diffuser inlet
2	at diffuser exit

[redacted]

HUB at blade hub

TIP at blade tip

RECIPROCATING-ENGINE INSTALLATION

The type of reciprocating-engine internal-flow system to be discussed is illustrated in figure 1. The air enters a plenum chamber through a screened inlet, proceeds through a fan and diffuser, and then splits into parallel streams. Each of the parallel ducts contains an air-using unit - such as the carburetor, the transmission-oil cooler, the engine-cylinder cooling ducts, and the engine-oil cooler. The air exhausted from these various units, with the exception of the carburetor, is then collected in a compartment containing an exit to atmosphere.

In typical existing systems of this type, the following characteristics generally apply: The inlets and exits are large and the intention is not to recover ram pressure at the inlet or thrust at the exit; the fan operates at engine speed and may or may not have contravanes; the engine cooling air flow requires 50 to 60 percent of the total internal air flow; and the rear compartment is not generally airtight.

The purpose of the following discussion is to determine whether there are particular methods of design and operation which will produce an appreciable saving in horsepower expenditure for the cooling system. An airtight system will be assumed, since it is impossible to determine drag quantities with indeterminate leakages. Before the effect of flight velocity is discussed, a review of the role of the cooling fan in the system is necessary.

The total power P in units of horsepower chargeable to the cooling system may be expressed as follows:

$$\sum P = \frac{Q\ \Delta H_F}{550\eta} + \frac{Q(\Delta H_C + \Delta H_D - \Delta H_F)}{550} + \frac{Q\rho}{550 \times 2}(V_O - V_X)^2$$

The preceding equation assumes no compressibility or heating effects but is sufficiently accurate for the application to be discussed. The first term on the right-hand side is the fan-shaft horsepower. The second term is, by definition, the "residual pumping" horsepower or the air-pumping power required to overcome total-pressure losses of the system in excess of the total-pressure rise supplied by the fan. The third term is the wake horsepower or power associated with kinetic energy left in the air after it is discharged to the atmosphere. The sum of the last two terms may be shown algebraically to correspond to the conventional equation for internal drag.

[redacted]

In order to illustrate the effect of the fan and duct losses on the total cooling horsepower, some simplified configurations are presented in figure 2, together with cooling-horsepower calculations for the case where the cooler total-pressure loss is equal to the fan total-pressure rise, which is equal to the flight dynamic pressure q_0. It is a familiar axiom that, for an efficient ducting system, if the cooling fan is designed just to overcome the system total-pressure losses, a minimum overall cooling-drag power results. This condition is represented by the configuration of figure 2(a), where the net total-pressure loss is zero and, thus, the only horsepower expenditure is the fan-shaft horsepower, $q_0Q/550\eta$. The configuration of figure 2(b), which consists of an inefficient duct without cooler or fan and with a total-pressure loss equal to q_0, requires an infinite exit area since the exit total pressure is equal to free-stream static pressure. Under these conditions, the exit velocity is essentially zero, and the sum of the residual-pumping and wake horsepowers is approximately twice the total cooling horsepower of the efficient cooling design (fig. 2(a)). Adding the fan and cooler to the configuration of figure 2(b) produces an inefficient cooling system (configuration of fig. 2(c)), which also has a net total-pressure loss equal to q_0. Figure 2 indicates that the total cooling horsepower for this system is approximately three times that of the efficient cooling system. With inefficient fan designs and air leaks, this value may be much higher. The excessive horsepower of the configuration of figure 2(c) results from the fact that total-pressure losses not compensated for by the fan produce penalties in horsepower twice - once in residual-pumping power and once in wake power.

In order to examine the cooling-horsepower problem further, particularly with regard to the effect of flight velocity on magnitudes, some calculations were made for the helicopter model of reference 1. The helicopter has the following specifications:

Gross weight, lb	10,000
Tip speed, fps	500
Solidity	0.07
Disk loading, lb/sq ft	2.5
Flat-plate parasite drag, sq ft	40
Rated engine power, hp	1,000

The curve for helicopter power required, calculated for level equilibrium flight, and the assumed fuel-air-ratio variation are given in figure 3. The system cooling requirements, which were estimated by assuming an air temperature of 100° F and parallel air circuits similar to that shown in figure 1, are presented in figure 4. The cooling-fan performance characteristics assumed on the basis of data in reference 2 are presented in figure 5. In matching the fan characteristics to the cooling requirements, the hovering condition was assumed to correspond to a Q/nD^3 of 0.3,

[redacted]

and the fan pressure rise for hovering was assumed to be 20 percent greater than the required cooling air pressure drop.

Some of the resulting cooling-horsepower calculations are shown in figure 6 as a function of flight speed V_0. The curves shown correspond to the condition where the correct amount of cooling air flow is obtained at each flight speed by controlling the exit area. The amount of horsepower has been referenced to the cooling horsepower required in hovering for the lowest curve. In current practice, this value of cooling horsepower (unity) may range between approximately 4 and 10 percent of the engine normal rated power. The curve shapes resemble the shape of the curve of engine horsepower required, as would be expected, except for the drop in cooling horsepower at the high-speed end. This effect is due to richer mixtures at high engine powers, since fuel cooling results and thus the air cooling requirements are reduced. In the two lower curves, an efficient duct system or 100-percent ram recovery was assumed. In the lowest curve, the fan efficiency was held constant at 75 percent, presumably by controlling some component of the fan geometry. In the middle curve, a typical variation of fan efficiency with volume flow was assumed; in other words, a fixed fan geometry. The advantage of variable fan geometry is indicated by figure 6 to be small (on the order of 5 to 10 percent). The top curve assumes an inefficient duct system or a complete loss of ram recovery. Complete loss of ram added 30 percent to the horsepower in the cruise range (90 mph) and doubled the power at about 120 mph, the rated horsepower condition. In addition, in the range of the dashed curve the exit areas required to obtain the necessary cooling air flows were over twice that which was considered a reasonable value. At the higher flight speeds now contemplated for helicopters, the increased cooling powers produced by loss of ram would be even larger.

Cooling-horsepower calculations for the condition of a fixed exit area equal to that required for the hovering condition are presented in figure 7. The curve of figure 6 for a fixed fan and controllable exit area is also given again for reference purposes. In the curve for 100-percent ram recovery, the fan just meets the cooling requirements in hovering. As the flight speed increases with a fixed exit area, the ram recovery forces more air through the system, so that the cooling requirements are exceeded and the horsepower is increased. This effect adds about 70 percent to the cooling horsepower in cruising and 50 percent at rated power. The effect would be larger for helicopters designed for higher flight speeds. Thus, it is seen that a controllable exit area is a powerful device for maintaining minimum cooling powers. To produce an effective exit-area control, however, leaks must be minimized.

The top curve of figure 7, because it corresponds to zero ram recovery and fixed exit area, is for a fixed air flow. Consequently, the curve indicates that, for a complete loss of ram, the wake and residual-pumping powers increase rapidly with increasing flight speed. The dashed portion of the curve corresponds to conditions where cooling is not quite adequate

because the required cooling air flow is slightly more for the rated-power condition than for the hovering condition. The fact that the two upper curves are almost coincident indicates that the cooling horsepower for a fixed exit-area design is not appreciably reduced by a high ram recovery.

In connection with the general problem of the design of cooling systems, a large amount of data is available in the literature and the more important references have been listed. References 3 to 17 contain diversified information including design procedures and fundamental concepts and have become basic references in this field. References 18 to 30, in general, contain data on specific configurations or aerodynamic effects in the low-speed or incompressible-flow range. References 31 to 41 are reports of investigations of diffusers and bends in which boundary-layer-control devices were evaluated. References 42 to 44 and reference 2 are useful in designing cooling fans.

TURBINE-ENGINE INSTALLATION

The conventional turbine engine with an axial-flow compressor is a convenient package unit of favorable aerodynamic shape with apparently a minimum of ducting complications. Investigations reported in references 45 to 51 and other unpublished data have indicated, however, that some engines of this type are sensitive to distortions in the air flow and pressure distribution at the face of the compressor. Some of the engines tested have exhibited very serious reductions in performance due to this effect.

Figure 8 outlines some of the effects on the individual engine components for one of the most distorted distributions investigated (ref. 45). The air-flow maldistribution was set up by the installation of a screen in one of the twin intake ducts, which resulted in a 62 percent to 38 percent distribution of the air flow and a pressure distortion just upstream from the compressor face of ±19 percent of the absolute pressure. The inlet pressure distortion was smoothed out by the compressor, and pressure distributions throughout the rest of the engine were approximately normal. A small distortion of ±5 percent was measured at the turbine exit. As a result of the unequal pressure ratios across the two halves of the compressor, a temperature distortion of +15 percent to -6 percent of the absolute temperature was present at the compressor outlet. These conditions led to a ±54-percent temperature distortion at the turbine inlet and ±6 percent at the turbine outlet. The compressor efficiency was lowered 17 percent; the combustion efficiency was unaffected; and an 8-percent reduction was obtained in the turbine efficiency. The net effect of these changes in the component performances was a loss in thrust of 26 percent and an increase in specific fuel consumption of 23 percent. Because of unfavorable effects on the compressor stall and surge characteristics, the engine operating range was curtailed. It should be emphasized

that the numbers given here are the maximum values observed over the operating range tested. An engine modified for helicopter application would be expected to produce similar results.

The seriousness of this problem in helicopter installations is difficult to predict. Helicopter air inlets are subject to operation over a very wide range of angle of attack and yaw and, therefore, may operate inefficiently. Siamese inlets, under some operating conditions, may set up large distortions due to the fact that one inlet may be recovering approximately full ram while the other is operating in the fuselage wake. It is difficult to imagine, however, that pressure distortions at the compressor face will approach the ±19-percent value shown in figure 8. Nevertheless, the penalties are so high that helicopter designers should attempt to minimize the effect.

One solution is to adapt the installation to the engine. This adaptation might be accomplished by feeding the compressor inlet from a plenum chamber similar to that used for conventional cooling installations of reciprocating engines. Another solution is to adapt the engine to the installation, which means employing engines insensitive to inlet irregularities - for instance, the centrifugal compressor-type engines.

HIGH-SPEED EFFECTS IN DUCTS

High subsonic flow velocities in duct elements, such as diffusers and bends, produce performances appreciably different from low subsonic velocities. These effects are probably due to increases in both Reynolds and Mach numbers; as yet, sufficient data are not available to isolate the two variables. Since high subsonic flow velocities are anticipated in some of the duct elements in turbine-engine installations and in pressure-jet-type powerplants, high-speed effects are of interest to helicopter designers.

Figure 9 presents some data for conical diffusers on the effect of speed on diffuser loss coefficient. The Mach number at station 1 has been selected as the index to speed. The diffuser area ratio is 2.0 and a moderate boundary-layer thickness was present at the inlet. The ratio of loss coefficient obtained at some inlet Mach number to the loss coefficient obtained at an inlet Mach number of 0.2 is given as a function of diffuser expansion angle, 2θ, for curves of constant inlet Mach number. The curves show that for short diffusers, expansion angle in the range of 20° to 24°, the loss coefficient at high subsonic Mach numbers may reach values approaching twice that corresponding to a Mach number

of 0.2. The increased total-pressure loss is, of course, accompanied by more distorted exit-velocity distributions. Additional data on these effects are given in references 52 to 63. Similar performance trends have been observed for flow around bends and are discussed in reference 64.

CHOKING MACH NUMBER FOR BENDS

In the design of pressure-jet systems, the maximum flow capacity of duct elements, especially bends, becomes of interest. The aerodynamic index to maximum flow capacity is the choking Mach number. Unpublished NACA data and other data from reference 64 are summarized in figure 10. Data are given for 90° bends of both circular and rectangular cross section. For the choking condition, the mean Mach number at the inlet reference station is given as a function of bend radius ratio. For the rectangular bends, curves of constant aspect ratio h/w are presented. An aspect ratio of 1.0 corresponds to a bend of square cross section. All the rectangular-bend data are for a very thin inlet boundary layer. The curve for the circular bends contains both thick and thin inlet-boundary-layer points.

All the curves indicate that reducing the radius ratio - in other words, increasing the sharpness of the turn - reduces the choking Mach number or flow capacity of the bend. For rectangular bends, the square cross section is optimum with higher or lower aspect ratios producing lower choking Mach numbers. The comparison of the circular and square bends shows the circular bend to be slightly superior. Thickening the boundary layer in the circular bend had no appreciable effect on the choking Mach number. A choking Mach number of 0.7, which is obtainable with the better configurations of figure 10, corresponds to 91 percent of the theoretical maximum weight flow obtainable at a Mach number of 1.0.

FLOW IN DUCTED ROTOR BLADE

In the design of pressure-jet-type systems, the aerodynamics of the flow through a ducted helicopter blade becomes important, both from the standpoint of the total-pressure losses involved and from the standpoint of flow conditions produced at the tip burner inlet. Figure 11 illustrates the effect of centrifugal force on the flow in a ducted helicopter blade. The calculations were made by using the one-dimensional expressions and analysis presented in reference 65. The calculations presented in figures 11 to 13 are for a completely insulated duct; therefore, the total temperature rises somewhat due to compression (adiabatic compression) as the flow proceeds from blade hub to tip. The preceding assumption differs from that used in the calculations of reference 65 where an

isothermal compression or constant total temperature was assumed. In the latter case, the heat lost through the duct walls would have to be just sufficient to counteract the tendency for the total temperature to rise due to compression. In the calculations presented herein, the adiabatic assumption was made because it produces more pessimistic answers relative to total-pressure losses and choking Mach number.

Figures 11, 12, and 13 were constructed on the further assumption that the ratio of the ducted-flow total temperature at the rotor hub to the free-stream ambient temperature is 1.0. The value of this ratio affects only the numerical values of rotor-tip Mach numbers identifying the curves of these figures. The curves may be made to correspond to another value of the temperature ratio by multiplying the given values of rotor-tip Mach number by the square root of the desired ratio.

A long straight duct at rest will choke at the exit if sufficient pressure drop is imposed on the flow. This case is illustrated by the dashed lines of figure 11, which, as indicated, correspond to zero rotor-tip Mach number. A single circular duct is illustrated; however, the analysis can be applied also to multiple ducts and to odd cross-sectional shapes. As the flow proceeds down the nonrotating duct, friction losses cause a progressive drop in total pressure accompanied by a dropping density, increasing dynamic pressure, and thus an increasing Mach number. The initial Mach number, 0.57, for the zero-rotation case illustrated, was chosen so as to produce a Mach number of 1.0 or choking at a duct length of 60 diameters. If the duct is rotated at some blade-tip Mach number, such as the 0.95 value in figure 11, the centrifugal forces oppose the friction effects and compress the flow. Since centrifugal force is directly proportional to the radius, the compression effect is not noticeable in a region adjacent to the hub, and the two cases illustrated in figure 11 produce approximately coincident total-pressure curves in this region. At duct lengths exceeding about 15 diameters, the centrifugal forces become predominant and a total-pressure ratio of about 1.35 is eventually attained. Correspondingly, the Mach number for the case with rotation rises initially because of friction effects, and then the curve peaks and starts to drop when the centrifugal effects become stronger. The initial Mach number, 0.77, was chosen so that the duct just choked at the location of the peak. It will be noted that, although the duct is choked, the final Mach number is relatively low, 0.52. The flow capacity of the duct has been appreciably increased by rotation as evidenced by the higher initial Mach number with rotation.

By calculating a number of curves similar to those of figure 11, a map of the net Mach number changes across a given duct length for a range of tip Mach numbers may be constructed. Such a map for a duct length of 60 diameters is presented in figure 12. The plot of figure 12 shows in more detail than figure 11 that increasing the rotor-tip Mach number while maintaining a constant Mach number at the hub decreases the

ducted-flow Mach number at the rotor tip. Also, increasing the rotor-tip Mach number increases the ducted-flow Mach number at the rotor hub corresponding to choking.

Total- and static-pressure ratios across the 60-diameter length of duct are presented in figure 13. The pressure ratios were calculated from the Mach number values of figure 12. The maximum total-pressure ratio for a given rotor-tip Mach number occurs with no flow (zero hub Mach number). Increasing the flow quantity produces a drop in total-pressure ratio as a result of increased friction losses. The case illustrated indicates that, for a duct length of 60 diameters, total-pressure ratios on the order of 1.8 are obtainable for a rotor-tip Mach number of 1.0.

CONCLUDING REMARKS

The following statements summarize the discussion of pertinent items relative to the design of internal-flow systems for helicopter propulsive units:

1. With regard to reciprocating-engine installations in helicopters designed for speeds above 100 mph, a high ram recovery and controllable exit area are required simultaneously in order to avoid excessive cooling-horsepower penalties.

2. The installation in helicopters of turbine engines with axial-flow compressors may be penalized by the sensitivity of some of these engines to velocity and pressure distortions at the compressor face. The use of a plenum chamber upstream from the compressor will aid in overcoming this effect.

3. Relative to the design of turbine-engine installations and pressure-jet systems, high subsonic speeds in duct elements, such as diffusers and bends, produce appreciable depreciation in performance.

4. Choking Mach number data on 90° bends of circular and square cross section indicate that flow capacities equal to 91 percent of the maximum theoretical value are obtainable.

5. Available one-dimensional relations for determining the effects of centrifugal forces on the flow in ducted helicopter rotors are shown to provide an evaluation of flow Mach numbers and pressure ratios.

Langley Aeronautical Laboratory,
National Advisory Committee for Aeronautics,
Langley Field, Va., June 11, 1954.

[redacted]

REFERENCES

1. Harrington, Robert D.: Reduction of Helicopter Parasite Drag. NACA TN 3234, 1954.

2. Bell, E. Barton: Test of a Single-Stage Axial-Flow Fan. NACA Rep. 729, 1942.

3. Rubert, Kennedy F. and Knopf, George S.: A Method for the Design of Cooling Systems for Aircraft Power-Plant Installations. NACA WR L-49, 1942. (Formerly NACA ARR, Mar. 1942.)

4. Becker, John V., and Baals, Donald D.: Analysis of Heat and Compressibility Effects in Internal Flow Systems and High-Speed Tests of a Ram-Jet System. NACA Rep. 773, 1943. (Supersedes NACA WR L-535.)

5. Henry, John R.: Design of Power-Plant Installations. Pressure-Loss Characteristics of Duct Components. NACA WR L-208, 1944. (Formerly NACA ARR L4F26.)

6. Rogallo, F. M.: Internal-Flow Systems for Aircraft. NACA Rep. 713, 1941.

7. Wood, George P., and Brevoort, Maurice J.: Design, Selection, and Installation of Aircraft Heat Exchangers. NACA WR L-341, 1943. (Formerly NACA ARR 3G31.)

8. Katzoff, S.: The Design of Cooling Ducts With Special Reference to the Boundary Layer at the Inlet. NACA WR L-321, 1940. (Formerly NACA ACR, Dec. 1940.)

9. Boelter, L. M. K., Morrin, E. H., Martinelli, R. C., and Poppendiek, H. F.: An Investigation of Aircraft Heaters. XIV - An Air and Heat Flow Analysis of a Ram-Operated Heater and Duct System. NACA WR W-21, 1944. (Formerly NACA ARR 4C01.)

10. Patterson, G. N.: Note on the Design of Corners in Duct Systems. R. & M. No. 1773, British A.R.C., 1937.

11. Patterson, G. N.: Corner Losses in Ducts. Aircraft Engineering, vol. IX, no. 102, Aug. 1937, pp. 205-208.

12. Abramovich, G.: Fluid Motion in Curved Channels. From Collection of Reports on Industrial Aerodynamics and Fan-Construction, Rep. No. 211 (text in Russian), Trans. Central Aero-Hydrodyn. Inst. (Moscow), 1935, pp. 97-151.

[redacted]

13. Patterson, G. N.: The Design of Aeroplane Ducts. Rules To Be Followed for the Reduction of Internal and External Drag. Aircraft Engineering, vol. XI, no. 125, July 1939, pp. 263-268.

14. Patterson, G. N.: Modern Diffuser Design. Aircraft Engineering, vol. X, no. 115, Sept. 1938, pp. 267-273.

15. Gibson, A. H.: On the Flow of Water Through Pipes and Passages Having Converging or Diverging Boundaries. Proc. Roy. Soc. (London), ser. A., vol. 83, no. 563, Mar. 2, 1910, pp. 366-378.

16. Becker, John V.: Wind-Tunnel Investigation of Air Inlet and Outlet Openings on a Streamline Body. NACA Rep. 1038, 1951. (Supersedes NACA WR L-300.)

17. Becker, John V., and Baals, Donald D.: High-Speed Tests of a Ducted Body With Various Air-Outlet Openings. NACA WR L-486, 1942. (Formerly NACA ACR, May 1942.)

18. Nelson, W. J., and Czarnecki, K. R.: Wind-Tunnel Investigation of Wing Ducts on a Single-Engine Pursuit Airplane. NACA WR L-407, 1943. (Formerly NACA ARR 3J13.)

19. Nelson, W. J., Czarnecki, K. R., and Harrington, Robert D.: Full-Scale Wind-Tunnel Investigation of Forward Underslung Cooling-Air Ducts. NACA WR L-115, 1944. (Formerly NACA ARR L4H15.)

20. Czarnecki, K. R., and Nelson, W. J.: Wind-Tunnel Investigation of Rear Underslung Fuselage Ducts. NACA WR L-438, 1943. (Formerly NACA ARR 3I21.)

21. Peters, H.: Conversion of Energy in Cross-Sectional Divergences Under Different Conditions of Inflow. NACA TM 737, 1934.

22. McLellan, Charles H., and Nichols, Mark R.: An Investigation of Diffuser-Resistance Combinations in Duct Systems. NACA WR L-329, 1942. (Formerly NACA ARR, Feb. 1942.)

23. Weske, John R.: Pressure Loss in Ducts With Compound Elbows. NACA WR W-39, 1943. (Formerly NACA ARR, Feb. 1943.)

24. Wirt, Loring: New Data for the Design of Elbows in Duct Systems. Gen. Elec. Rev., vol. 30, no. 6, June 1927, pp. 286-296.

25. McLellan, Charles H., and Bartlett, Walter A., Jr.: Investigation of Air Flow in Right-Angle Elbows in a Rectangular Duct. NACA WR L-328, 1941. (Formerly NACA ARR, Oct. 1941.)

[redacted]

26. Kröber, G.: Guide Vanes for Deflecting Fluid Currents With Small Loss of Energy. NACA TM 722, 1933.

27. Nichols, Mark R.: Investigation of Flow Through an Intercooler Set at Various Angles to the Supply Duct. NACA WR L-408, 1942. (Formerly NACA ARR, Apr. 1942.)

28. Reid, Elliott G.: Performance Characteristics of Plane-Wall Two-Dimensional Diffusers. NACA TN 2888, 1953.

29. Squire, H. B.: Experiments on Conical Diffusers. Rep. No. Aero 2216, British R.A.E., Aug. 1947.

30. Squire, H. B., and Carter, P.: Further Experiments on Conical Diffusers. Rep. No. 13,499, British A.R.C., Nov. 6, 1950.

31. Biebel, William J.: Low-Pressure Boundary-Layer Control in Diffusers and Bends. NACA WR L-84, 1945. (Formerly NACA ARR L5C24.)

32. Gratzer, L. B., and Smith, R. H.: Boundary Layer Control for Wide Angle Diffusers. Rep. No. 300 (ONR Contract N6ori-217, Task Order I, Project No. NR-061-004), Univ. Washington Aero. Lab., Nov. 22, 1948.

33. Valentine, E. Floyd, and Carroll, Raymond B.: Effects of Some Primary Variables of Rectangular Vortex Generators on the Static-Pressure Rise Through a Short Diffuser. NACA RM L52B13, 1952.

34. Valentine, E. Floyd, and Carroll, Raymond B.: Effects of Several Arrangements of Rectangular Vortex Generators on the Static-Pressure Rise Through a Short 2:1 Diffuser. NACA RM L50L04, 1951.

35. Wood, Charles C.: Preliminary Investigation of the Effects of Rectangular Vortex Generators on the Performance of a Short 1.9:1 Straight-Wall Annular Diffuser. NACA RM L51G09, 1951.

36. Wood, Charles C., and Higginbotham, James T.: The Influence of Vortex Generators on the Performance of a Short 1.9:1 Straight-Wall Annular Diffuser With a Whirling Inlet Flow. NACA RM L52L01a, 1953.

37. Wood, Charles C., and Higginbotham, James T.: Flow Diffusion in a Constant-Diameter Duct Downstream of an Abruptly Terminated Center Body. NACA RM L53D23, 1953.

38. Wood, Charles C., and Higginbotham, James T.: Performance Characteristics of a 24° Straight-Outer-Wall Annular-Diffuser—Tailpipe Combination Utilizing Rectangular Vortex Generators for Flow Control. NACA RM L53H17a, 1953.

[redacted]

39. Henry, John R., and Wilbur, Stafford W.: Preliminary Investigation of the Flow in an Annular-Diffuser—Tailpipe Combination With an Abrupt Area Expansion and Suction, Injection, and Vortex-Generator Flow Controls. NACA RM L53K30, 1954.

40. Valentine, E. Floyd, and Copp, Martin R.: Investigation To Determine Effects of Rectangular Vortex Generators on the Static-Pressure Drop Through a 90° Circular Elbow. NACA RM L53G08, 1953.

41. Taylor, H. D.: Application of Vortex Generator Mixing Principle to Diffusers. Concluding Report. Air Force Contract W33-038 ac-21825. U.A.C. Rep. R-15064-5, United Aircraft Corp. Res. Dept., Dec. 31, 1948.

42. Schulze, Wallace M., Erwin, John R., and Ashby, George C., Jr.: NACA 65-Series Compressor Rotor Performance With Varying Annulus-Area Ratio, Solidity, Blade Angle, and Reynolds Number and Comparison With Cascade Results. NACA RM L52L17, 1953.

43. Kahane, A.: Charts of Pressure Rise Obtainable With Airfoil-Type Axial-Flow Cooling Fans. NACA TN 1199, 1947.

44. Mutterperl, William: High-Altitude Cooling. VI - Axial-Flow Fans and Cooling Power. NACA WR L-776, 1944. (Formerly NACA ARR L4I11e.)

45. Wallner, Lewis E., Conrad, E. William, and Prince, William R.: Effect of Uneven Air-Flow Distribution to the Twin Inlets of an Axial-Flow Turbojet Engine. NACA RM E52K06, 1953.

46. Conrad, E. William, and Sobolewski, Adam E.: Investigation of Effects of Inlet-Air Velocity Distortion on Performance of a Turbojet Engine. NACA RM E50G11, 1950.

47. Sanders, Newell D., and Palasics, John: Analysis of Effects of Inlet Pressure Losses on Performance of Axial-Flow Type Turbojet Engine. NACA RM E8J25b, 1948.

48. Huppert, Merle C.: Preliminary Investigation of Flow Fluctuations During Surge and Blade Row Stall in Axial-Flow Compressors. NACA RM E52E28, 1952.

49. Bullock, Robert O., Wilcox, Ward W., and Moses, Jason J.: Experimental and Theoretical Studies of Surging in Continuous-Flow Compressors. NACA Rep. 861, 1946.

50. Mark, Herman, and Zettle, Eugene V.: Effect of Air Distribution on Radial Temperature Distribution in One-Sixth Sector of Annular Turbojet Combustor. NACA RM E9I22, 1950.

[redacted]

51. Childs, J. Howard, McCafferty, Richard J., and Surine, Oakley W.: Effect of Combustor-Inlet Conditions on Performance of an Annular Turbojet Combustor. NACA Rep. 881, 1947.

52. Copp, Martin R., and Klevatt, Paul L.: Investigation of High-Subsonic Performance Characteristics of a 12° 21-Inch Conical Diffuser, Including the Effects of Change in Inlet-Boundary-Layer Thickness. NACA RM L9H10, 1950.

53. Persh, Jerome: The Effect of the Inlet Mach Number and Inlet-Boundary-Layer Thickness on the Performance of a 23° Conical-Diffuser - Tail-Pipe Combination. NACA RM L9K10, 1950.

54. Little, B. H., Jr., and Wilbur, Stafford W.: High-Subsonic Performance Characteristics and Boundary-Layer Investigations of a 12° 10-Inch-Inlet-Diameter Conical Diffuser. NACA RM L50C02a, 1950.

55. Copp, Martin R.: Effects of Inlet Wall Contour on the Pressure Recovery of a 10° 10-Inch-Inlet-Diameter Conical Diffuser. NACA RM L51E11a, 1951.

56. Nelson, William J., and Popp, Eileen G.: Performance Characteristics of Two 6° and Two 12° Diffusers at High Flow Rates. NACA RM L9H09, 1949.

57. Young, A. D., and Green, G. L.: Tests of High-Speed Flow in Diffusers of Rectangular Cross-Section. British R. & M. No. 2201, British A.R.C., 1944.

58. Persh, Jerome, and Bailey, Bruce M.: The Effect of Various Arrangements of Triangular Ledges on the Performance of a 23° Conical Diffuser at Subsonic Mach Numbers. NACA TN 3123, 1954.

59. Persh, Jerome, and Bailey, Bruce M.: A Method for Estimating the Effect of Turbulent Velocity Fluctuations in the Boundary Layer on Diffuser Total-Pressure-Loss Measurements. NACA TN 3124, 1954.

60. Persh, Jerome: The Effect of Surface Roughness on the Performance of a 23° Conical Diffuser at Subsonic Mach Numbers. NACA RM L51K09, 1952.

61. Bohm, H., and Koppe, M.: The Influence of Friction on Steady Diffuser Flows at High Speed. Joint Intelligence Objectives Agency (Washington), July 23, 1946. (Also available from CADO, Wright-Patterson Air Force Base, as ATI No. 36689.)

62. Naumann: Wirkungsgrad von Diffusoren bei hohen Unterschallgeschwindigkeiten. FB Nr. 1705, Deutsche Luftfahrtforschung (Berlin-Adlershof), 1942.

63. Froessel, W.: Investigation of Compressible Flow on and Near a Curved Profile. AAF Translation No. F-TS-1517-RE, Air Materiel Command, U.S. Army Air Forces, Aug. 1947.

64. Young, A. D., Green, G. L., and Owen, P. R.: Tests of High-Speed Flow in Right-Angled Pipe Bends of Rectangular Cross-Section. British R. & M. No. 2066, British A.R.C., 1943.

65. Henry, John R.: One-Dimensional, Compressible, Viscous Flow Relations Applicable to Flow in a Ducted Helicopter Blade. NACA TN 3089, 1953.

[redacted]

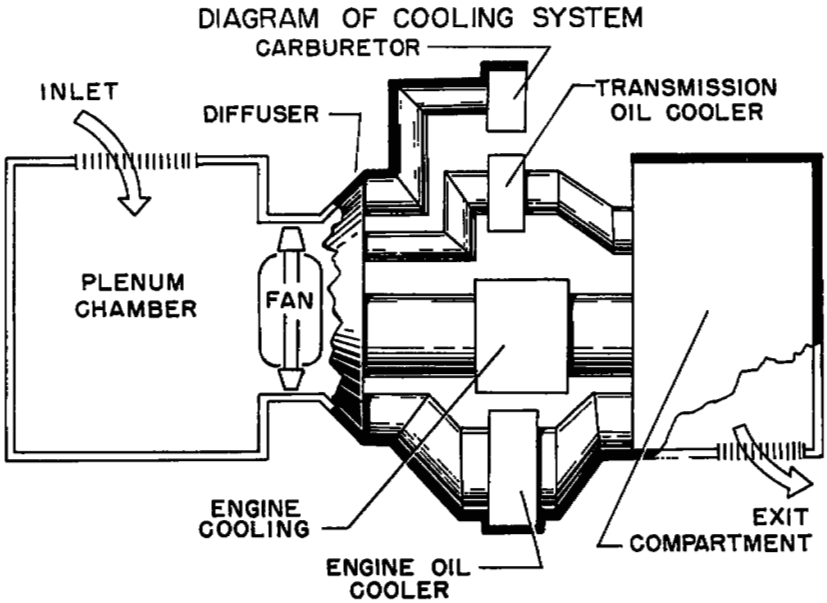

Figure 1

BREAKDOWN OF COOLING HP FOR CASE OF $q_0 = \Delta H_C = \Delta H_F$

CONFIGURATION	FAN SHAFT HP RESIDUAL PUMPING HP WAKE HP TOTAL COOLING HP
(a) EFFICIENT DESIGN FAN, COOLER; V_0 → V_0; NET $\Delta H = 0$	$q_0Q/550\,\eta$ 0 0 $q_0Q/550\,\eta$
(b) INEFFICIENT DUCT NO FAN OR COOLER; V_0 → $V \approx 0$; $\Delta H = q_0$	0 $q_0Q/550$ $q_0Q/550$ $2q_0Q/550$
(c) COMBINATION FAN, COOLER; V_0 → $V \approx 0$; NET $\Delta H = q_0$	$q_0Q/550\,\eta$ $q_0Q/550$ $q_0Q/550$ $>3q_0Q/550$

Figure 2

[redacted]

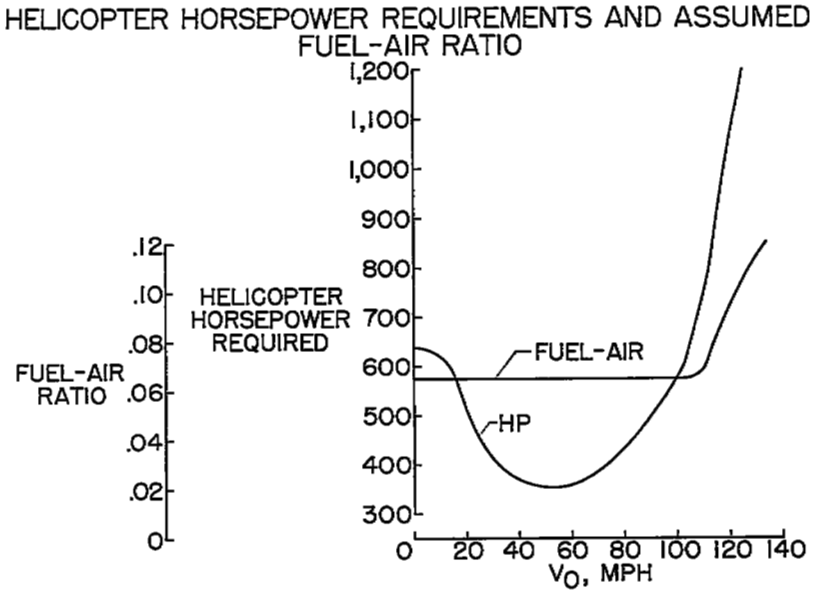

Figure 3

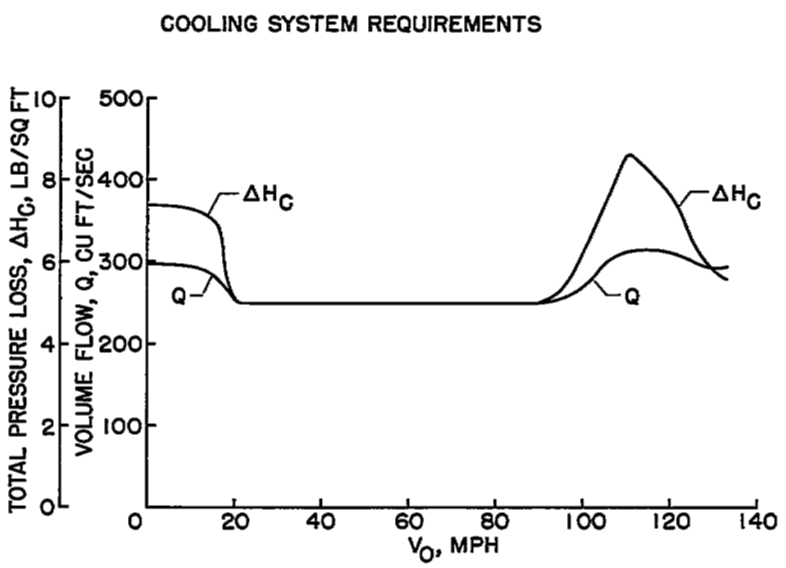

Figure 4

[redacted]

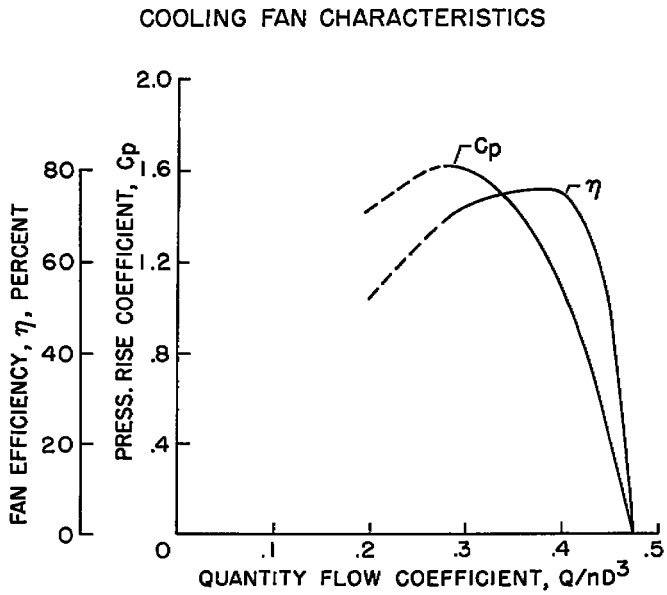

Figure 5

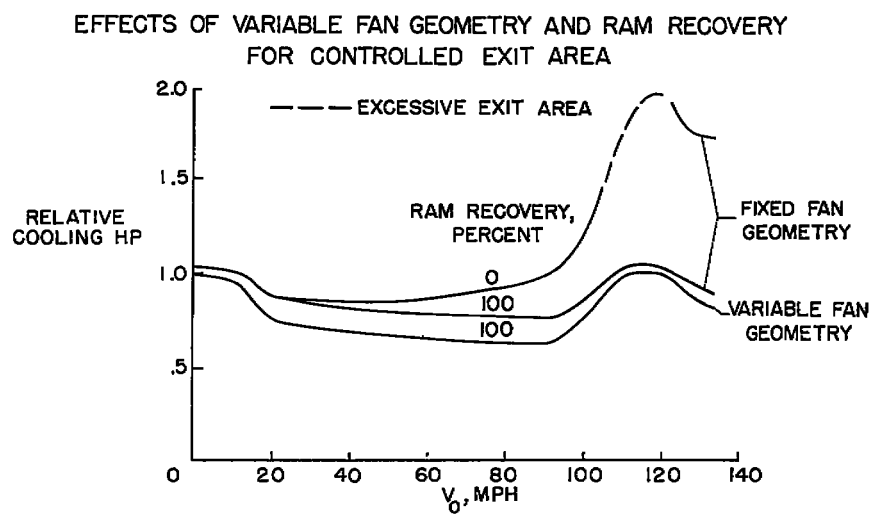

Figure 6

[redacted]

EFFECT OF RAM RECOVERY FOR FIXED EXIT AREA
AND FIXED FAN GEOMETRY

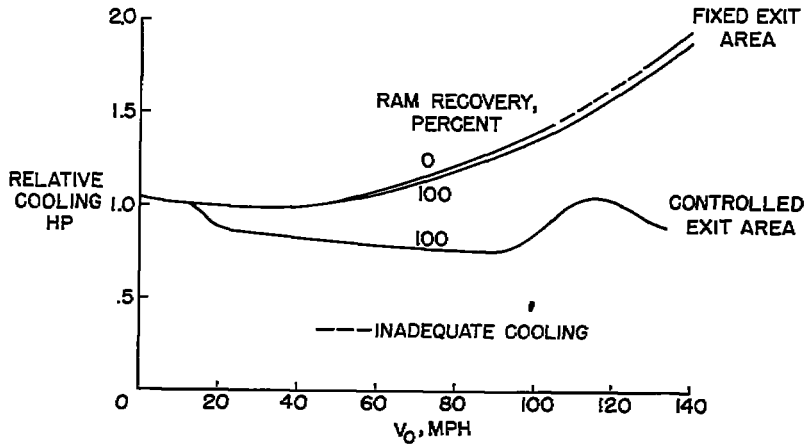

Figure 7

MAXIMUM PERFORMANCE REDUCTIONS DUE TO INLET AIR
MALDISTRIBUTION IN TURBINE ENGINE

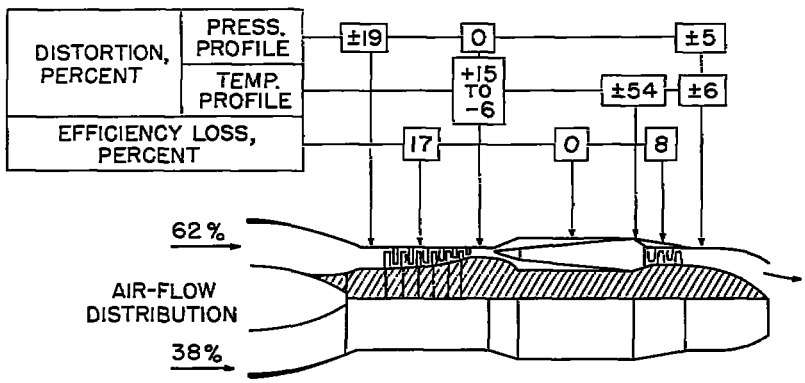

LOSS IN THRUST = 26 %
INCREASE IN SPECIFIC FUEL = 23%
ENGINE OPERATING RANGE CURTAILED

Figure 8

VARIATION OF CONICAL-DIFFUSER LOSS COEFFICIENT WITH MACH NUMBER

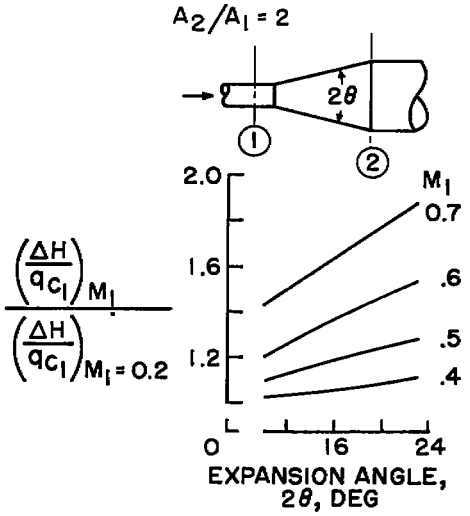

Figure 9

CHOKING MACH NUMBER FOR 90° BENDS

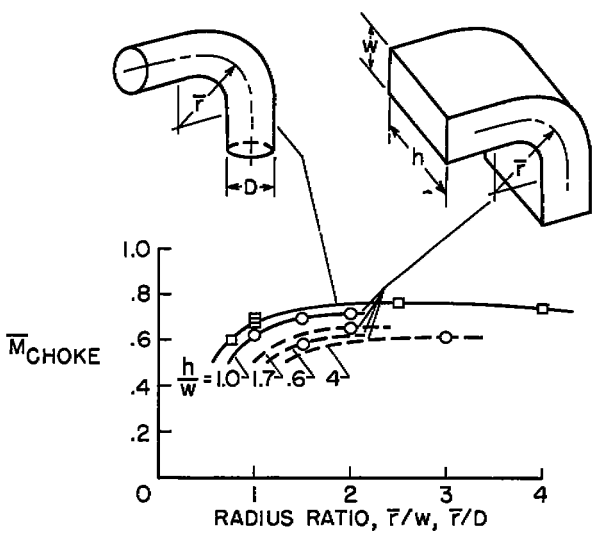

Figure 10

[redacted]

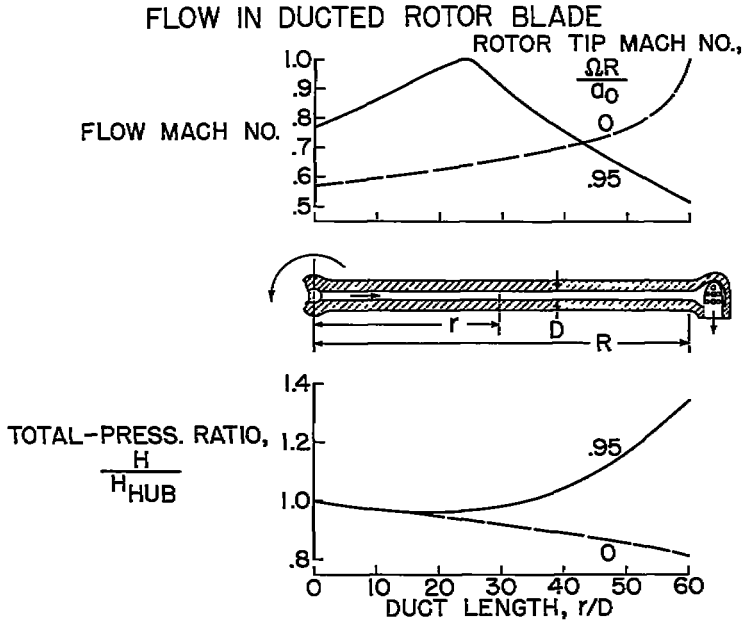

Figure 11

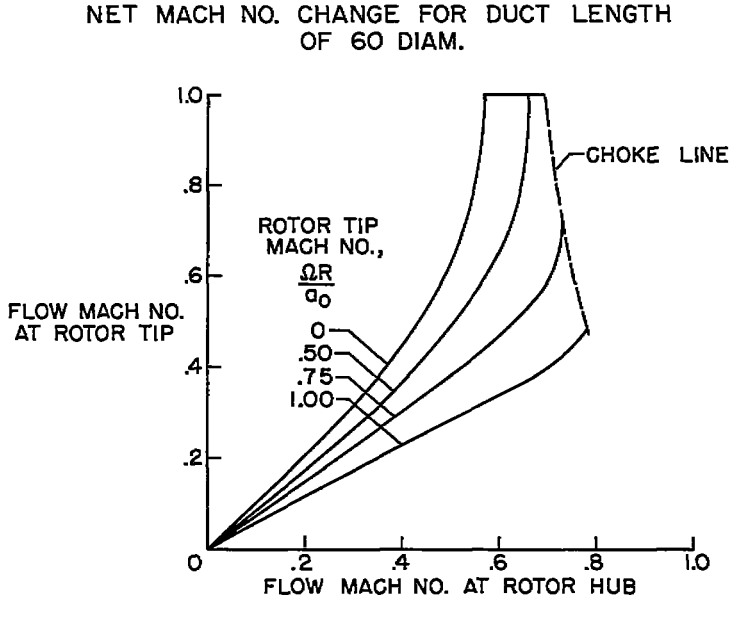

Figure 12

[redacted]

TOTAL- AND STATIC-PRESSURE RATIOS FOR DUCT LENGTH OF 60 DIAM.

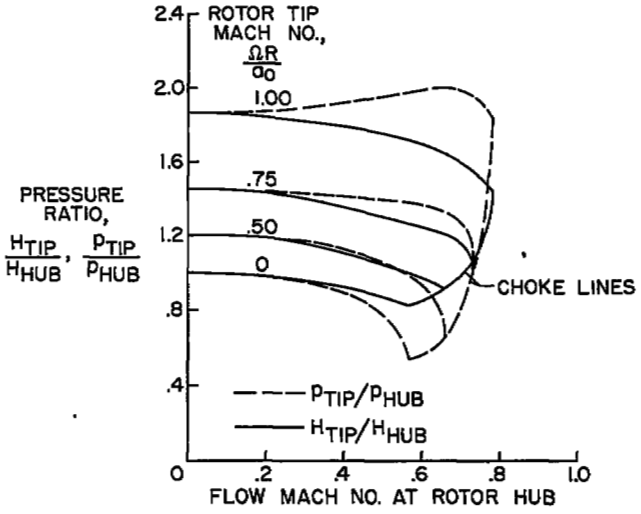

Figure 13

NACA-Langley - 9-14-54 - 350